

A functional screen identifies *hDRIL1* as an oncogene that rescues RAS-induced senescence

Daniel S. Peeper*, Avi Shvarts*, Thijn Brummelkamp*, Sirith Douma*, Eugene Y. Koh†, George Q. Daley† and René Bernards*‡

*Division of Molecular Carcinogenesis and Center for Biomedical Genetics, The Netherlands Cancer Institute, Plesmanlaan 121, 1066 CX Amsterdam, The Netherlands

†Whitehead Institute for Biomedical Research, 9 Cambridge Center, Cambridge, Massachusetts 02142, USA

‡e-mail: bernards@nki.nl

Published online: 28 January 2002, DOI: 10.1038/ncb742

Primary fibroblasts respond to activated H-RAS^{V12} by undergoing premature arrest, which resembles replicative senescence¹. This irreversible 'fail-safe mechanism' requires p19^{ARF}, p53 and the *Retinoblastoma* (*Rb*) family: upon their disruption, RAS^{V12}-expressing cells fail to undergo senescence and continue to proliferate¹⁻⁷. Similarly, co-expression of oncogenes such as c-MYC or E1A rescues RAS^{V12}-induced senescence. To identify novel genes that allow escape from RAS^{V12}-induced senescence, we designed an unbiased, retroviral complementary DNA library screen. We report on the identification of *DRIL1*, the human orthologue of the mouse *Bright* and *Drosophila dead ringer* transcriptional regulators. *DRIL1* renders primary murine fibroblasts unresponsive to RAS^{V12}-induced anti-proliferative signalling by p19^{ARF}/p53/p21^{CIP1}, as well as by p16^{INK4a}. In this way, *DRIL1* not only rescues RAS^{V12}-induced senescence but also causes these fibroblasts to become highly oncogenic. Furthermore, *DRIL1* immortalizes mouse fibroblasts, in the presence of high levels of p16^{INK4a}. Immortalization by *DRIL1*, whose product binds the pRB-controlled transcription factor E2F1 (ref. 8), is correlated with induction of E2F1 activity. Correspondingly, *DRIL1* induces the E2F1 target *Cyclin E1*, overexpression of which is sufficient to trigger escape from senescence. Thus, *DRIL1* disrupts cellular protection against RAS^{V12}-induced proliferation downstream of the p19^{ARF}/p53 pathway.

RAS^{V12}-induced premature senescence resembles replicative senescence, which occurs upon explantation of primary cells and is unrelated to the 'senescence crisis' that is caused by telomere loss. To identify novel genes that allow a bypass of RAS^{V12}-induced senescence, we designed an unbiased, functional genetic screen. After retrovirus-mediated expression of RAS^{V12}, more than 99.9% of a primary mouse embryo fibroblast (MEF) population underwent premature senescence, but a few cells escaped (most likely because of endogenous mutations) and continued to proliferate. To reduce this 'background' in the screen, we generated conditionally immortalized MEFs, co-expressing a temperature-sensitive simian virus 40 (SV40) large T mutant⁹ and RAS^{V12}. These 'BTR' cells proliferated indefinitely at 32 °C but became senescent at 39.5 °C owing to both the rapid disappearance of large T antigen (A.S., T.B., E.Y.K., G.Q.D. and R.B., unpublished observations) and the presence of RAS^{V12}. Indeed, the number of background colonies

was greatly reduced by using this system (Fig. 1a).

We screened a replication-deficient high-complexity retroviral complementary DNA library, prepared from JEG3 human chorion carcinoma cells, which yielded ~200 colonies (see Methods for details). DNA sequencing of two independent proviral inserts isolated from rescued colonies revealed that they originated from the same human gene, *DRIL1* (ref. 10). The murine orthologue of *DRIL1*, *Bright*, encodes a B-cell transcription factor that binds to the matrix-associated region (MAR) of the IgH locus¹¹. The product of the *Drosophila* orthologue of *DRIL1*, *dead ringer* (*dri*)¹², is a potent transcriptional repressor required for the recruitment of Groucho to Dorsal¹³.

Retroviral expression of epitope-tagged *DRIL1* confirmed that it conferred a transformed phenotype on BTR cells at the non-permissive temperature (Fig. 1b, upper panel). The same was observed for its murine orthologue, *Bright*, which has 80% amino acid identity overall, excluding the possibility that human *DRIL1* acts as a dominant-negative in murine cells (data not shown). The senescence bypass became most apparent 2–3 weeks after infection, when the control cells had become completely senescent and the *DRIL1*-expressing cells proliferated rapidly (not shown). Importantly, primary MEFs, too, were rescued from RAS^{V12}-induced senescence by *DRIL1* (Fig. 1c), morphologically transformed (Fig. 1b, lower panel) and no longer contact-inhibited (Fig. 1d). Moreover, MEFs co-expressing *DRIL1*/RAS^{V12} efficiently

Table 1 MEFs co-expressing *DRIL1*/RAS^{V12} are oncogenic

Cells	Tumour induction	Latency period (days)
HA- <i>DRIL1</i>	0/4	–
HA- <i>DRIL1</i> /RAS ^{V12} I	6/6	10
HA- <i>DRIL1</i> /RAS ^{V12} II	6/6	10
RAS ^{V12} /p19 ^{ARF} -/-	4/4	7

Nude, athymic mice were injected subcutaneously in both flanks with 10⁶ MEFs expressing cDNAs as indicated. Two independent clones of *DRIL1*/RAS^{V12} cells were analysed. Results are numbers of tumours per injection, 2 weeks after injection. *DRIL1*-expressing MEFs did not form tumours after 3 months.

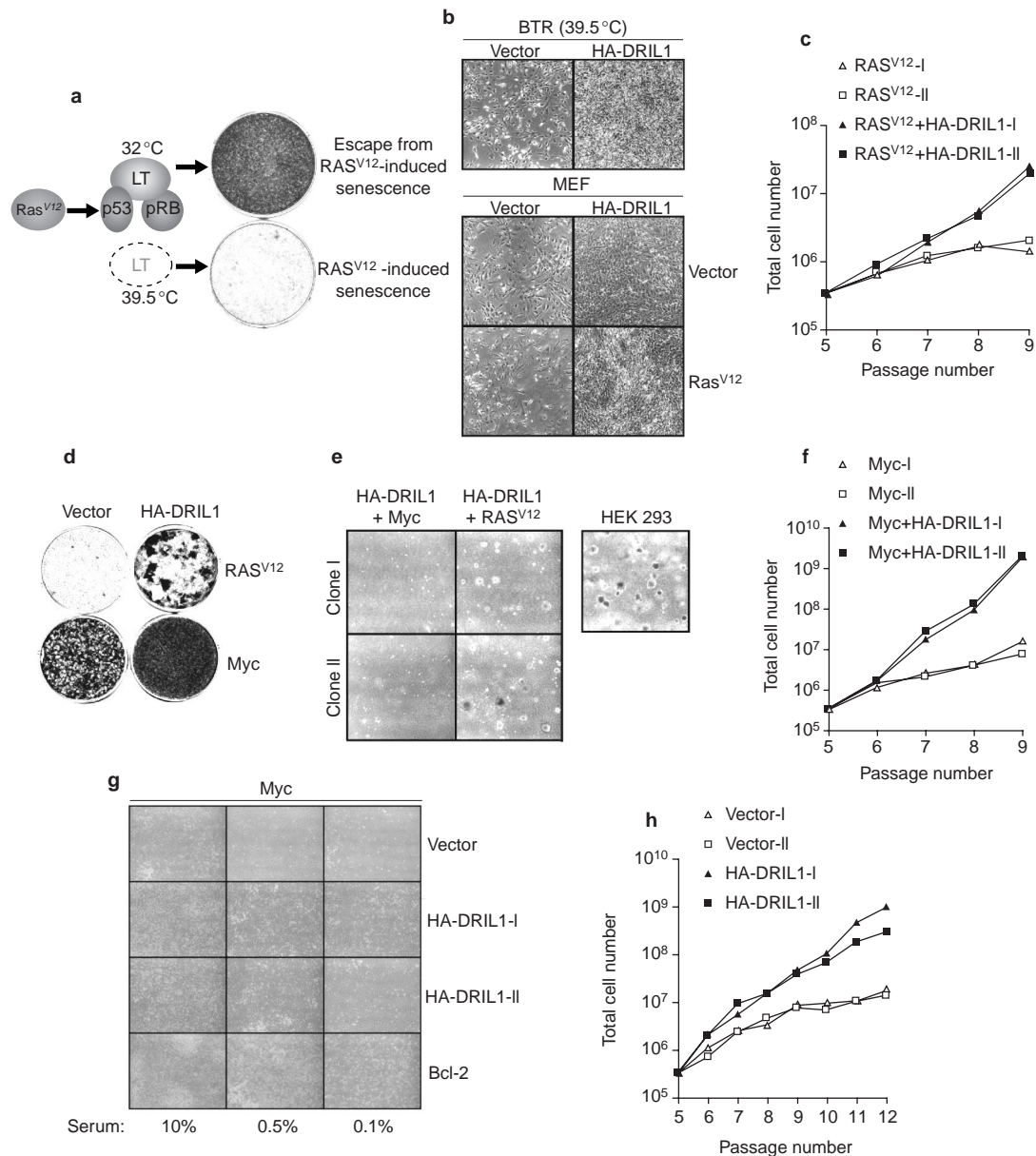


Figure 1 DRIL1 bypasses normal and Ras^{V12}-induced senescence in primary mouse fibroblasts. **a**, Functional screen system. Premature senescence of 'tsT' MEFs (of BALB/c genetic background) that express a temperature-sensitive mutant of SV40 large T antigen (LT) were used to generate a cell population stably expressing Ras^{V12} (BTR cells). These cells proliferate rapidly at the permissive temperature (32 °C) but undergo premature senescence at the restrictive temperature (39.5 °C). **b**, DRIL1-dependent morphological transformation of BTR cells and MEFs, in the context of Ras^{V12}. BTR cells (upper panel) or normal, primary MEFs (of OLA genetic background; lower panel) were infected with retroviruses expressing either no insert or HA-DRIL1. After 2 d, the BTR cells were shifted to the non-permissive temperature. Two weeks later, the BTRs and MEFs were photographed at $\times 40$ magnification. **c**, DRIL1 bypasses Ras^{V12}-induced senescence. Normal, primary MEFs (of OLA genetic background) at passage 3 were (co-)infected with retroviruses, as indicated. At 2 d after infection, successfully infected cells were selected for 5 d for the expression of specific selectable markers encoded by the retroviruses (puromycin and/or hygromycin) and used in a proliferation curve. The proliferation curve was

initiated when the MEFs were at passage 5, which is close to the end of their normal life span. For each sample, duplicate data points were collected. **d**, DRIL1/Ras^{V12}-expressing fibroblasts fail to undergo contact-inhibition. MEFs were infected and selected as in **c** and used for a focus formation assay. The cells were left and reseeded on tissue culture plates for 3 weeks, then fixed and stained with crystal violet. **e**, DRIL1/Ras^{V12}-expressing fibroblasts proliferate independently of anchorage. MEFs were infected and selected as in **c** and seeded into soft agar. Adenovirus E1-transformed human embryonal kidney (HEK 293) cells served as a positive control. After 2 weeks, foci were photographed at $\times 40$ magnification. **f**, DRIL1 and c-Myc cooperate in accelerating proliferation. MEFs were infected, selected and used in a proliferation curve, as in **c**. **g**, DRIL1 reduces sensitivity to c-myc-induced apoptosis. MEFs were infected and selected as in **c**. They were then maintained in medium with a reduced serum concentration, as indicated. Cells were photographed at $\times 40$ magnification 1 week later. **h**, DRIL1 bypasses spontaneous senescence. MEFs (of OLA genetic background) were infected, selected and used in a proliferation curve, as in **c**.

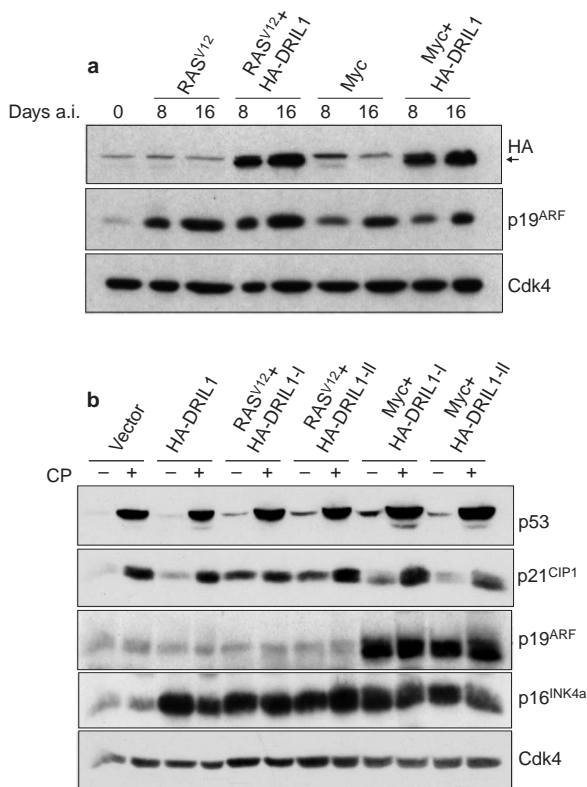


Figure 2 DRIL1 bypasses Ras^{V12}-induced senescence with intact p16^{INK4a}/p19^{ARF}/p53/p21^{CIP1} signalling. **a**, Primary MEFs (of OLA genetic background) at passage 3 were (co)-infected with retroviruses, as indicated. At 8 and 16 days after infection (a.i.), cell extracts were prepared and equal amounts were used for western blotting with the indicated antibodies. HA-DRIL1 (indicated by an arrow) runs slightly below a background band. **b**, Passage 4 wild-type MEFs and passage 20 stable DRIL1-expressing MEF clones (in either the absence or the presence of RAS^{V12} or c-MYC) were treated with cis-platin (CP; 50 μM). Cell extracts were prepared 16 h later and subjected to western blotting, with the indicated antibodies. Cdk4 served as a loading control.

grew anchorage-independently, a hallmark *in vitro* of oncogenic transformation (Fig. 1e). Indeed, two independent clones of MEFs expressing DRIL1/RAS^{V12}, but not of MEFs expressing only DRIL1, formed tumours in nude mice within 2 weeks, with only a slightly longer latency than RAS^{V12}-expressing p19^{ARF}^{-/-} MEFs (Table 1). This raises the possibility that DRIL1, on overexpression, might act as an oncogene also in humans. Preliminary experiments indicate that DRIL1 protein is relatively highly expressed in a number of human colon tumour cell lines (D.S.P., S.D. and R.B., unpublished observations), but it remains to be determined whether this also occurs in primary lesions.

DRIL1 also collaborated strongly with c-Myc in accelerating proliferation (Fig. 1f), correlating with a reduced tendency to undergo cell death after prolonged serum deprivation (Fig. 1g). In contrast to MEFs co-expressing DRIL1/RAS^{V12}, however, these cells remained contact-inhibited and failed to grow independently of anchoring (Fig. 1d, e).

Importantly, DRIL1 expression was sufficient to allow also primary MEFs to escape from spontaneous senescence (Fig. 1h; see also Fig. 1b, lower panel, and Fig. 4a, b). We have been culturing various lines of DRIL1-expressing MEFs for over three months, without any signs of either a decrease in proliferative rate or an onset of senescence (data not shown; see also below).

RAS^{V12}-induced senescence requires an intact p19^{ARF} locus^{2,3}. RAS^{V12} expression alone in wild-type MEFs led to an induction of

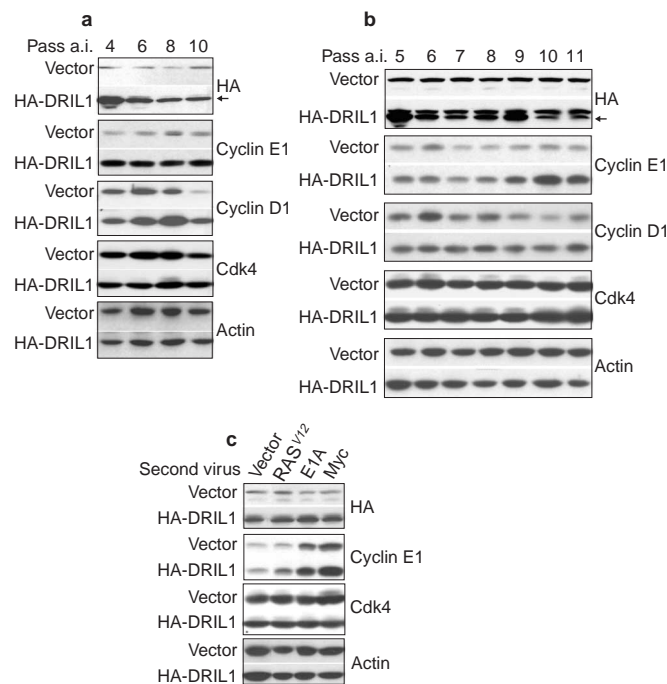


Figure 3 DRIL1-mediated bypass of spontaneous and Ras^{V12}-induced senescence is correlated with the induction of cyclin E1. **a**, **b**, BTR cells (**a**) or normal, primary MEFs (**b**) were infected with, and selected for expression of, retroviruses expressing either no insert or HA-DRIL1. After 2 d, the BTR cells were shifted to, and further maintained at, the non-permissive temperature. Both BTRs and MEFs were subjected to a 3T3-like protocol, in which they were split twice a week. At the indicated passage numbers after infection (pass. a.i.), cell extracts were prepared and subjected to western blotting with the indicated antibodies. **c**, MEFs were (co)-infected with retroviruses, as indicated. At 10 days after infection, cell extracts were prepared and subjected to western blotting with the indicated antibodies. The samples within each panel were analysed on the same gel but are represented in this way to permit a better comparison of the different time points. Actin served as a loading control for all blots.

p19^{ARF}, which persisted for up to at least 16 d after infection (Fig. 2a) but reproducibly declined to baseline levels thereafter (data not shown). Clearly, co-expression of DRIL1 did not interfere at all with this transient RAS^{V12}-dependent induction of p19^{ARF}. Likewise, late-passage DRIL1-expressing and DRIL1/RAS^{V12}-expressing MEF clones produced levels of p19^{ARF} that were similar to those in wild-type MEFs and thus had not selected against p19^{ARF} expression (Fig. 2b). This is in striking contrast to the BMI1 and TBX2 proteins, which bypass senescence by downregulating p19^{ARF} (ref. 14). Moreover, all DRIL1-expressing cells expressed high levels of the other INK4a locus-encoded regulator of senescence, p16^{INK4a} (Fig. 2b). Thus, none of the DRIL1-expressing cell populations had lost the expression of p19^{ARF} (or p16^{INK4a}) during the course of the senescence bypass and immortalization, in contrast with normal fibroblasts, which undergo spontaneous immortalization². Furthermore, DRIL1 did not prevent the induction of p19^{ARF}/p53/p21^{CIP1} by another 'mitogenic, stress-inducing protein', c-Myc (ref. 15), in both short-term and long-term experiments (Fig. 2a, b), despite the rapid proliferation of these cells (see Fig. 1f).

In addition to p19^{ARF}, p53 is also required for RAS^{V12}-induced senescence¹. We therefore determined whether DRIL1 (either in the presence or in the absence of mutant RAS) interfered with the basal levels, the regulation and/or the function of p53 and one of its transcriptional targets, p21^{CIP1}. The basal level of p21^{CIP1}, and to a smaller

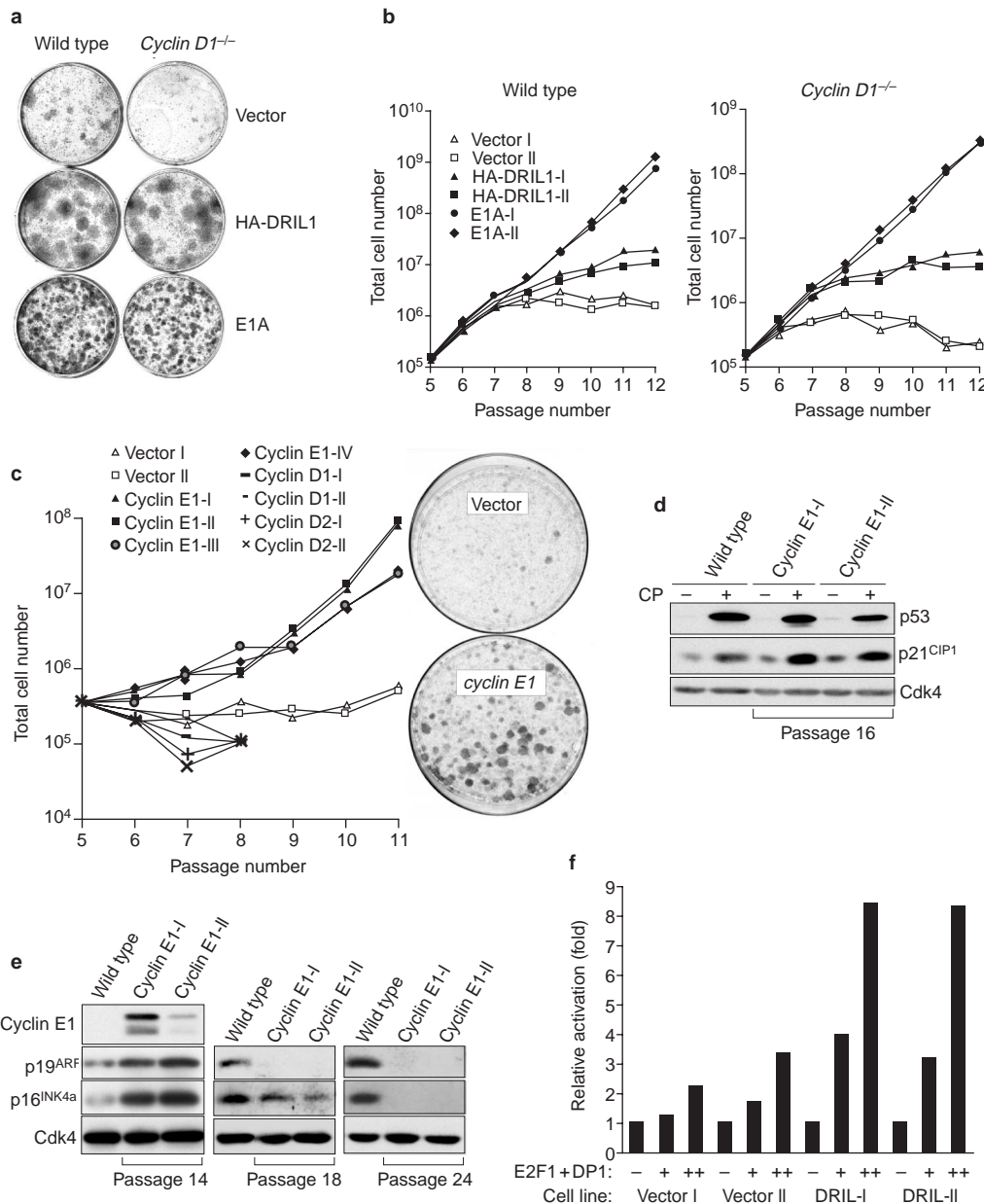


Figure 4 DRIL1-induced E2F1-cyclin-E1 signalling contributes to senescence bypass. **a, b,** Cyclin D1 is not required for DRIL1-dependent senescence bypass. Either wild-type or *Cyclin D1*^{-/-} MEFs, derived from littermates (of C57/BL6 genetic background), were infected with retroviruses, as indicated. They were then used both in a colony formation assay (**a**) and in a proliferation curve, as described in Fig. 1c. **(b)** The E1A-infected cells in **a** were fixed and stained 9 d after infection, and the remaining cells at 16 d after infection. **c,** Passage 1 MEFs (of OLA genetic background) were infected with the indicated retroviruses, selected and used either in proliferation curves (left-hand panel), as described in Fig. 1c, or in a colony-formation assay (right-hand panel). **d,** Two independent populations of passage-16 cyclin E1-immortalized MEFs, as well as low-passage wild-type MEFs, were treated with *cis*-platin (50 μM). Cell extracts were prepared 16 h later and equal amounts were subjected to western blotting with the indicated antibodies. **e,** Cell extracts

were prepared from two independent, cyclin E1-immortalized MEF clones at different passages, as indicated. Equal amounts of cell extract were subjected to western blotting with the indicated antibodies. Because retrovirally transduced cyclin E1 is of human origin (and was detected here with a human-specific antibody), it is impossible to determine its level of expression relative to endogenous mouse cyclin E1. Cdk4 served as a loading control. **f,** Independent 3T3 cell pools, stably expressing either empty vector or DRIL1, as indicated, were electroporated with an E2F-responsive firefly luciferase reporter plasmid (carrying six synthetic E2F1 consensus sites), as well as increasing amounts (0, 10 or 50 ng) of expression plasmids encoding E2F1 and its heterodimeric partner DP1. Represented is the activation of the reporter, relative to a co-introduced cytomegalovirus (CMV)-*Renilla* luciferase internal control, and normalized to the reporter activity in the absence of E2F1 + DP1. Averages from two independent experiments are shown.

extent that of p53, was markedly upregulated in MEFs expressing *DRIL1/RAS*^{V12} (which proliferate rapidly; see Fig. 1c) relative to young control MEFs (Fig. 2b). This occurred in spite of normal p19^{ARF} levels, which can be explained by a combination of the slight

induction of p21^{CIP1} by DRIL1 and the induction of p21^{CIP1} by *RAS*^{V12} in a partly p19^{ARF}-independent manner¹⁶. Apparently, DRIL1, in the context of *RAS*^{V12}, renders cells unresponsive to elevated levels of p21^{CIP1}. Next, we treated two independent late-passage

DRIL1-expressing and *DRIL1/RAS^{V12}*-expressing MEF clones with the DNA-damaging drug *cis*-platin and monitored the activation of p53 and p21^{CIP1}. This led to a significant induction of p53 in all clones, irrespective of *DRIL1* expression (Fig. 2b). Moreover, p53 was functional and active in these cells, as judged by the concomitant increase in p21^{CIP1} levels (Fig. 2b). Similar observations were made for treatment with ionizing radiation and for 3T3 cells stably expressing *DRIL1* (data not shown). Taken together, these results demonstrate that *DRIL1* bypasses both normal and *RAS^{V12}*-induced senescence without interfering with the (up)regulation of four critical senescence regulators, p19^{ARF}, p53, p21^{CIP1} and p16^{INK4a}, indicating that *DRIL1* acts downstream (or independent) of them during the immortalization of mouse fibroblasts in culture. Thus, remarkably, *DRIL1*-expressing cells and *Rb*-family-deficient cells⁷ share two important properties: on the one hand they show the normal signalling responses after expression of *RAS^{V12}*; on the other, they fail to show the normal biological response in that instead of undergoing replicative arrest, they continue to proliferate. These data raise the possibility that *DRIL1* interferes with pRB-dependent signalling.

To identify *DRIL1* target(s), other than the candidates discussed above, during the bypass of normal and *RAS^{V12}*-induced senescence, we made a comprehensive expression analysis of various cell-cycle-regulatory proteins in three experimental systems. First, we used the BTR cells in which we had identified *DRIL1* in the functional screen. Of many proteins analysed, two, cyclins D1 and E1, were found to be specifically upregulated by *DRIL1* during continued proliferation at the nonpermissive temperature (Fig. 3a). Second, during *DRIL1*-mediated immortalization of MEFs, we found a gradual upregulation of both cyclin E1 levels (but no marked effects on cyclin D1 abundance (Fig. 3b)) and cyclin E1-associated kinase activity (data not shown). Importantly, the induction of cyclin E1 in *DRIL1*-expressing MEFs occurred at about passage 9 (Fig. 3b). This was well correlated with the moment that the control MEFs underwent senescence, whereas the *DRIL1*-expressing fibroblasts continued to proliferate without delay (Fig. 1h). Third, in short-term co-infection experiments, the upregulation of cyclin E1 by *c-Myc* and E1A, and to a smaller extent by *RAS^{V12}*, was enhanced by *DRIL1* (Fig. 3c). Apparently, *DRIL1* can also upregulate cyclin E1 in cells in which *RAS^{V12}*-induced senescence is blocked. Taken together, these observations indicate that these cyclins are candidate proteins for either being required for or contributing to the *DRIL1*-mediated senescence bypass.

To determine whether cyclin D1 represents an essential mediator of *DRIL1* immortalization, we infected either wild-type or *Cyclin D1^{-/-}* MEFs with *DRIL1*-encoding retroviruses and monitored their proliferative potential. As with adenovirus E1A (which immortalizes cells downstream of cyclin D1, by sequestering pRB-family proteins), we observed an identical senescence-bypassing capacity of *DRIL1*, whether cyclin D1 was present or absent, in two independent assays (Fig. 4a, b). Thus, *DRIL1* bypasses the senescence of primary fibroblasts in a cyclin D1-independent manner, which is consistent with our observation that *DRIL1*-expressing MEFs are not sensitive to high levels of p16^{INK4a} (Fig. 2b).

We then introduced either D-type or E-type cyclins by retroviral transduction into primary MEFs and monitored whether the deregulated expression of either allowed a bypass of senescence. Deregulated expression of either *CYCLIN D1* or *CYCLIN D2* did not immortalize MEFs (Fig. 4c). By contrast, overexpression of *CYCLIN E1* (Fig. 4e, left panel) prevented MEFs from undergoing senescence, as shown for four independent MEF populations (Fig. 4c). We have cultured these cells for over 3 months without any signs of senescence (data not shown; see below). Two independent passage-14 *CYCLIN E1*-expressing MEF populations showed normal expression of both p19^{ARF} and p16^{INK4a}, relative to control MEFs (Fig. 4e, left-hand panel). However, after prolonged culturing these cells gradually decreased their levels of p19^{ARF} and p16^{INK4a} (Fig. 4e, middle and right-hand panels), for a currently unknown

reason. Importantly, downregulation of p19^{ARF} and p16^{INK4a} expression occurred after passage 14 (Fig. 4e), whereas the cells clearly escaped from senescence at about passage 8 (Fig. 4c), making it unlikely that these two events are functionally linked. The observation that *CYCLIN E1*-expressing MEFs at passage 18 expressed p16^{INK4a}, but no longer p19^{ARF}, suggests that this was not due to genetic loss of the entire *INK4a* locus but instead suggests an epigenetic phenomenon. A similar observation has been made recently for immortalization of bone marrow-derived macrophages¹⁷. Moreover, when we exposed late-passage *CYCLIN E1*-expressing MEFs to DNA damage, both clones induced high levels of p53, which was functional because it induced p21^{CIP1} (Fig. 4d). In conclusion, overexpression of *CYCLIN E1* is sufficient to trigger escape from senescence, at the least, without requiring the disruption of p16^{INK4a}/p19^{ARF}/p53/p21^{CIP1} signalling. Our observation that cyclin D1 is not required for *DRIL1* to bypass senescence fits well with the reported hierarchy of D- and E-type cyclins (where D precedes E in phosphorylating pRB (ref. 18) and with the observed resistance of *DRIL1* cells to elevated levels of p16^{INK4a} (which inhibits proliferation in an Rb-family-dependent manner). Collectively, these results indicate strongly that cyclin E1 represents an important *DRIL1* target, which conceivably contributes to its immortalizing activity. However, it is probably not the sole target, because *DRIL1* is a transcription factor that is expected to regulate a variety of genes. For example, it remains to be determined whether cyclin E1 can also interfere with *c-Myc*-induced cell death, as we observe for *DRIL1*. Consistent with the idea that cyclin E1 collaborates with the effects of *DRIL1*, overexpression of cyclin E1 collaborates with mutant *RAS* in the oncogenic transformation of primary rodent cells, as well as in tumorigenicity in mice^{19,20}. Although overexpression might not reflect the normal physiological role of cyclin E1, the relevance of our finding might become evident only during pathological situations, because the overexpression of *CYCLIN E1* has been observed in, and might contribute to, the emergence of human tumours²¹.

Deficiency in either p19^{ARF} or p53, but also in the Rb family, leads to a bypassing of both normal and *RAS^{V12}*-induced senescence^{6,7,22}. Moreover, the *CYCLIN E1* promoter is regulated by pRB/E2F1 (ref. 23), indicating that E2F1 might mediate the communication between *DRIL1* and Cyclin E1. Indeed, in two independent *DRIL1*-expressing 3T3 populations (which had identical cell cycle profiles to their parental counterparts and expressed functional p53 (data not shown)), E2F1 activated transcription to a markedly greater extent than in control cells (Fig. 4f). These results show that in the context of *DRIL1*, E2F1 has greater transcriptional activity, indicating that E2F1 is a prime candidate for involvement in the communication between *DRIL1* and cyclin E1. Consistent with this view is the previous isolation of *DRIL1* as an E2F1-associated protein, and the demonstration that it induces its transactivation potential through direct binding⁸, providing a possible explanation for the increase in cyclin E1 levels shown here. Moreover, our preliminary experiments reveal that, in contrast with murine cells, *DRIL1* induces premature senescence in primary human cells (data not shown). Strikingly, this property of *DRIL1* is shared by E2F1 (ref. 24). Although E2F1, like *DRIL1*, cooperates with mutant *RAS* in the transformation of primary rodent cells²⁵ as well as in skin tumour development in transgenic mice²⁶, it induces premature senescence in primary human cells²⁴. This observation is therefore also consistent with our view that *DRIL1* deregulates the pRB/E2F1 pathway, which apparently has different outcomes in murine and human cells. Finally, our findings are in agreement with and extend previous reports indicating that either cyclin E1 or E2F1 can bypass an ectopically induced p16^{INK4a} arrest^{27,28} and that cyclin E1–Cdk2 is pivotal in both *c-Myc*-dependent proliferation²⁹ and immortalization³⁰. Taken together, our results indicate strongly that *DRIL1* bypasses senescence downstream of the p19^{ARF}/p53 pathway by deregulating the p16^{INK4a}/pRB/E2F1 pathway. This notion is consistent with our earlier finding that genetic ablation of multiple *Rb*-family members renders cells insensitive to (*RAS^{V12}*-induced) p19^{ARF}/p53 signalling^{7,22}. □

Methods

Retroviral cDNA screen

BTR cells were generated by infection of *tsT* MEFs (of BALB/c origin; A.S., T.B., E.Y.K., G.Q.D. and R.B., unpublished observations) with *RAS*^{V12}-encoding retroviruses. These cells (7×10^5), maintained at the permissive temperature (32 °C), were infected twice with a high-complexity retrovirus cDNA library prepared from human JEG3 chorion carcinoma cells, in the presence of $5 \mu\text{g ml}^{-1}$ Polybrene (1,5-dimethyl-1,5-diazaundecamethylene polymethobromide; Sigma). At 2 d after infection, the cells were split 1:3 and, after attachment to the cell-culture plates, were shifted to the restrictive temperature (39.5 °C). Colonies started to appear after 7–10 d and were picked 2–3 weeks after infection. To discriminate between spontaneous colonies and colonies rescued by a retrovirally encoded cDNA, we superinfected individually established primary clones with wild-type murine Moloney leukaemia virus. Thus, proviral inserts were provided with the essential retroviral components such that recombinant retroviruses were produced and secreted into the culture medium¹⁴. The cell-free medium was subsequently used to infect fresh BTR cells, and another round of screening was performed. From each primary clone, 5–10 secondary clones were isolated and analysed further by Southern blotting with a provirus-specific 'sup F' probe, polymerase chain reaction (PCR) with retrovirus-specific primers, and DNA sequencing, to determine the number of proviral integrations and to isolate and identify them respectively. After proviral mobilization of 20 primary clones with wild-type Moloney virus, at least 5 also appeared positive in the second round of screening, indicating that the biological activity was carried by a transferable element rather than being caused by an endogenous mutation in the BTR fibroblasts.

PCR and construction of human and murine *DRIL1* expression vectors

DNA sequencing of two PCR fragments, derived from two independent primary colonies (and conserved in their respective secondary colonies), revealed that they encoded the same cDNA, *hDRIL1*. These cDNAs initiated at 162 and 173 base pairs, respectively, downstream of the reported translation start site¹⁰. In both cDNAs, use of the first subsequent in-frame ATG gives rise to a protein lacking its amino-terminal 58 amino acids. To isolate a full-length cDNA, we performed a PCR on JEG3 cDNA with primers specific for the 5' and 3' termini of the *DRIL1* cDNA. The integrity of the PCR product was confirmed by sequencing both strands. Both the original, cloned cDNA and the full-length cDNA were identical to the published sequence¹⁰, except for a carboxy-terminal stretch where Gly₅Ser₃ in the reported sequence (residues 599–608) was replaced by Gly₆Ser₄. The significance of this difference, which maps to a non-conserved region, is unknown. The full-length cDNA was provided with a haemagglutinin (HA)-epitope-encoding tag and cloned into (pBABE retroviral) expression vectors. To isolate a full-length *Bright* cDNA, we performed PCR on a mouse-embryo cDNA library with primers specific for its 5' and 3' termini and subsequently cloned the cDNA into a pBABE retroviral expression vector.

Cell culture, retroviral infection and proliferation curves

MEFs of OLA genetic background (for either *DRIL1* or Cyclin E1 proliferation curves) were isolated as described previously⁷ and maintained in DMEM (Gibco) supplemented with 10% fetal bovine serum (PAA Laboratories) and 0.1 mM 2-mercaptoethanol. *Cyclin D1*^{-/-} MEFs and MEFs derived from littermates were kindly provided by Dr. P. Sicinski (Boston, Massachusetts) and of C57/Bl6 genetic background. Phoenix packaging cells were used to generate ecotropic retroviruses and the retroviral cDNA library, as described¹. MEFs were infected with filtered (pore size 0.45 μm) viral supernatant, supplemented with 4–8 $\mu\text{g ml}^{-1}$ Polybrene. In general, a single infection round of 6 h was sufficient to infect at least 90% of the population.

For proliferation curves, passage-1–3 MEFs were infected in one to three sequential rounds with pBABE retroviral vectors carrying selectable markers⁵; at 1 or 2 days after infection they were selected with puromycin (1–3 $\mu\text{g ml}^{-1}$) or hygromycin (50 $\mu\text{g ml}^{-1}$) for at least 5 days. After confirmation that all mock-infected cells were dead, the cells were seeded at a density of 1.5×10^5 cells per 5-cm plate and subjected to a 3T3-like protocol, in which they were split twice a week. The proliferation curve was initiated when the MEFs were at passage 5, which is close to the end of their normal lifespan. For each sample, at least duplicate datapoints were collected.

Soft agar assays and tumour growth in mice

Cells were infected and selected briefly as described for the proliferation curves. Cells were used for either assay 6 d after infection. To monitor the capacity of MEFs to grow in semi-solid medium *in*

vitro, cells were transferred to 2 ml complete DMEM containing 0.4% low-gelling agarose (Sigma type VII, catalogue no. A-4018). Then, 2.5×10^4 cells were seeded in duplicate into six-well plates containing a 2-ml layer of solidified 1% agar in complete medium. The number of foci was determined 2 weeks later. For analysis of the tumorigenic capacity of MEFs *in vivo*, athymic nude mice were injected subcutaneously in each flank with 10^6 cells; mice were inspected weekly. Mice were killed at the time that tumours reached a diameter of 10 mm.

Antibodies

The following antibodies were used for western blotting: M-156 for p16^{INK4a}, C-19 for p21^{CIP1}, C-22 for CDK4, H-295 for cyclin D1, C-19 for human cyclin E1, and C-11 for actin (all from Santa Cruz); Ab7 for p53 (from Calbiochem); R-562 for p19^{ARF} and 12CA5 for HA (both from Abcam).

RECEIVED 17 MAY 2001; 5 SEPTEMBER 2001; ACCEPTED 26 OCTOBER 2001;
PUBLISHED 28 JANUARY 2002.

- Serrano, M., Lin, A. W., McCurrach, M. E., Beach, D. & Lowe, S. W. *Cell* **88**, 593–602 (1997).
- Kamijo, T. *et al. Cell* **91**, 649–659 (1997).
- Palmero, I., Pantoja, C. & Serrano, M. *Nature* **395**, 125–126 (1998).
- Sherr, C. J. *Genes Dev.* **12**, 2984–2991 (1998).
- Tanaka, N. *et al. Cell* **77**, 829–839 (1994).
- Sage, J. *et al. Genes Dev.* **14**, 3037–3050 (2000).
- Peepker, D. S., Dannenberg, J. H., Douma, S., te Riele, H. & Bernards, R. *Nature Cell Biol.* **3**, 198–203 (2001).
- Suzuki, M. *et al. Oncogene* **17**, 853–865 (1998).
- Lee, G. H., Ogawa, K. & Drinkwater, N. R. *Am. J. Pathol.* **147**, 1811–1822 (1995).
- Kortschak, R. D. *et al. Genomics* **51**, 288–292 (1998).
- Herrscher, R. F. *et al. Genes Dev.* **9**, 3067–3082 (1995).
- Gregory, S. L., Kortschak, R. D., Kalionis, B. & Saint, R. *Mol. Cell. Biol.* **16**, 792–799 (1996).
- Kortschak, R. D., Tucker, P. W. & Saint, R. *Trends Biochem. Sci.* **25**, 294–299 (2000).
- Kamijo, J. J. *et al. Nature Genet.* **26**, 291–299 (2000).
- Zindy, F. *et al. Genes Dev.* **12**, 2424–2433 (1998).
- Pantoja, C. & Serrano, M. *Oncogene* **18**, 4974–4982 (1999).
- Randle, D. H., Zindy, F., Sherr, C. J. & Roussel, M. F. *Proc. Natl Acad. Sci. USA* **98**, 9654–9659 (2001).
- Lundberg, A. S. & Weinberg, R. A. *Mol. Cell. Biol.* **18**, 753–761 (1998).
- Haas, K. *et al. Oncogene* **15**, 2615–2623 (1997).
- Karsunky, H. *et al. Oncogene* **18**, 7816–7824 (1999).
- Keyomarsi, K. & Herliczek, T. W. *Prog. Cell Cycle Res.* **3**, 171–191 (1997).
- Dannenberg, J. H., van Rossum, A., Schuijff, L. & te Riele, H. *Genes Dev.* **14**, 3051–3064 (2000).
- Ohtani, K., DeGregori, J. & Nevins, J. R. *Proc. Natl Acad. Sci. USA* **92**, 12146–12150 (1995).
- Dimri, G. P., Itahana, K., Acosta, M. & Campisi, J. *Mol. Cell. Biol.* **20**, 273–285 (2000).
- Johnson, D. G., Cress, W. D., Jakoi, L. & Nevins, J. R. *Proc. Natl Acad. Sci. USA* **91**, 12823–12827 (1994).
- Pierce, A. M., Fisher, S. M., Conti, C. J. & Johnson, D. G. *Oncogene* **16**, 1267–1276 (1998).
- Lukas, J., Petersen, B. O., Holm, K., Bartek, J. & Helin, K. *Mol. Cell. Biol.* **16**, 1047–1057 (1996).
- Alevizopoulos, K., Vlach, J., Hennecke, S. & Amati, B. *EMBO J.* **16**, 5322–5333 (1997).
- O'Hagan, R. C. *et al. Genes Dev.* **14**, 2185–2191 (2000).
- Groth, A., Weber, J. D., Willumsen, B. M., Sherr, C. J. & Roussel, M. F. *J. Biol. Chem.* **275**, 27473–27480 (2000).

ACKNOWLEDGEMENTS

We thank C. Sherr for generously providing *ARF*^{-/-} MEFs, N. Drinkwater for the *tsT*-antigen plasmid, P. Sicinski for *Cyclin D1*^{-/-} MEFs, G. Nolan for retroviral packaging cells, T. van Wezel for invaluable help with PCR, J. van der Sman for help with analysis of the screen, H. Starreveld and the animal facility for help with oncogenicity assays, P. Tucker for reagents and for sharing unpublished observations, our colleagues for helpful discussions, and A. Berns, R. Agami, R. Kortlever and B. Rowland for reading the manuscript critically. This work was supported by grants from the Dutch Cancer Society, the Human Frontiers Science Program (HFSP) and the National Institutes of Health (USA). G.D. is the Birnbaum Scholar of the Leukemia and Lymphoma Society of America and a recipient of a Burroughs Wellcome Career Award in the Biomedical Sciences.

Correspondence and requests for materials should be addressed to R.B.